JACC: CARDIOVASCULAR IMAGING VOL. 6, NO. 4, 2013

ISSN 1936-878X/$36.00
PUBLISHED BY ELSEVIER INC. http://dx.doi.org/10.1016/j.jcmg.2012.10.023

Low-Dose Dual-Source CT Angiography With Iterative Reconstruction for Coronary Artery Stent Evaluation

Jasmin Eisentopf, MD,* Stephan Achenbach, MD,† Stefan Ulzheimer, PhD,‡ Christian Layritz, MD,* Wolfgang Wuest, MD,§ Matthias May, MD,§ Michael Lell, MD,§ Dieter Ropers, MD,* Lutz Klinghammer, MD,* Werner G. Daniel, MD,* Tobias Pflederer, MD*

Erlangen, Giessen, and Forchheim, Germany

OBJECTIVES The purpose of this study was to evaluate the image quality and diagnostic accuracy of very low-dose, dual-source computed tomography (DSCT) angiography for the evaluation of coronary stents.

BACKGROUND Iterative reconstruction (IR) leads to substantial reduction of image noise and hence permits the use of very low-dose data acquisition protocols in coronary computed tomography angiography.

METHODS Fifty symptomatic patients with 87 coronary stents (diameter 3.0 ± 0.4 mm) underwent coronary DSCT angiography (heart rate, 60 ± 6 beats/min; prospectively electrocardiography-triggered axial acquisition; 80 kV, 165 mA, 2 × 128 × 0.6-mm collimation; 60 ml of contrast at 6 ml/s) before invasive coronary angiography. DSCT images were reconstructed using both standard filtered back projection and a raw data–based IR algorithm (SAFIRE, Siemens Healthcare, Forchheim, Germany). Subjective image quality (4-point scale from 0 [nondiagnostic] to 3 [excellent image quality]), image noise, contrast-to-noise ratio as well as the presence of in-stent stenosis >50% were independently determined by 2 observers.

RESULTS The median dose-length product was 23.0 (22.0; 23.0) mGy · cm (median estimated effective dose of 0.32 [0.31; 0.32] mSv). IR led to significantly improved image quality compared with filtered back projection (image quality score, 1.8 ± 0.6 vs. 1.5 ± 0.5, $p < 0.05$; image noise, 70 Hounsfield units [62; 80 Hounsfield units] vs. 96 Hounsfield units [82; 113 Hounsfield units], $p < 0.001$; contrast-to-noise ratio, 11.0 [9.6; 12.4] vs. 8.0 [6.2; 9.3], $p < 0.001$). To detect significant coronary stenosis in filtered back projection reconstructions, the sensitivity, specificity, positive predictive value, and negative predictive value were 97% (32 of 33), 53% (9 of 17), 80% (32 of 40), and 90% (9 of 10) per patient, respectively; 89% (43 of 48), 79% (120 of 152), 57% (42 of 74), and 96% (121 of 126) per vessel, respectively; and 85% (12 of 14), 69% (51 of 73), 32% (11 of 34), and 96% (51 of 53) per stent, respectively. In reconstructions obtained by IR, the corresponding values were 100% (33 of 33), 65% (11 of 17), 85% (33 of 39), and 100% (11 of 11) per patient, respectively; 96% (46 of 48), 84% (129 of 152), 66% (47 of 71), and 98% (127 of 129) per vessel, respectively; and 100% (14 of 14), 75% (55 of 73), 44% (14 of 32), and 100% (55 of 55) per stent, respectively. These differences were not significant.

CONCLUSIONS In selected patients, prospectively electrocardiography-triggered image acquisition with 80-kV tube voltage and low current in combination with IR permits the evaluation of patients with implanted coronary artery stents with reasonable diagnostic accuracy at very low radiation exposure. (J Am Coll Cardiol Img 2013;6:458–65) © 2013 by the American College of Cardiology Foundation

Temporal and spatial resolution of computed tomography (CT) has improved substantially during the past decade. Although applications of coronary CT angiography have become more widespread, the clinical utility of coronary CT angiography to identify in-stent stenosis remains questionable. This is partly due to the wide range of sensitivity (between 86% and 95% in recent studies) and specificity (between 84% and 98%) as well as the often low positive predictive value in published comparisons between CT angiography and invasive coronary angiography (1–6). In addition, the radiation exposure associated with coronary CT angiography remains of concern (7,8). New image acquisition protocols, such as the use of prospectively triggered axial acquisition, and advanced iterative image reconstruction techniques permit substantial reductions in radiation exposure (9–13). Iterative reconstruction (IR) may furthermore improve image quality (14–16).

Low-dose coronary CT angiography with IR has been demonstrated to allow high accuracy for the detection of coronary artery stenoses, but its value for the identification of in-stent stenosis has so far not been assessed. We therefore investigated a series of 50 patients with previously implanted coronary artery stents, scheduled for invasive coronary angiography, who underwent dual-source CT (DSCT) coronary angiography before invasive catheterization.

METHODS

Patient population. Fifty consecutive patients with previous coronary stent implantation (87 stented lesions) referred for invasive coronary angiography due to suspected progression of coronary artery disease were included in the study.

Patients with impaired renal function (serum creatinine >1.5 mg/dl), with known allergy to a contrast agent, or who were possibly pregnant as well as patients in non–sinus rhythm or acute coronary syndromes were not included in the study. Stent-specific exclusion criteria were previous stent-in-stent implantation and previous stent implantation in bifurcation lesions or bypass grafts. All included patients gave written informed consent, and the study was approved by the institutional review board.

All patients with a heart rate >65 beats/min received 100 mg of atenolol orally 45 to 60 min before the DSCT examination. If the heart rate in inspiration remained >65 beats/min at the time of the scan, as many as 4 doses of 5 mg metoprolol were given intravenously to reach a target heart rate <60 beats/min. Patients who did not reach the target heart rate were not excluded. All patients received 0.8-mg isosorbide dinitrate sublingually before DSCT examination.

DSCT data acquisition. All patients were examined while in the supine position during inspiratory breath-hold using a DSCT system (Somatom Definition Flash, Siemens Healthcare, Forchheim, Germany) with a gantry rotation time of 0.28 s. Tube voltage was set to 80 kV, and tube current was 165 mA. DSCT datasets were simultaneously acquired in 2 × 128 slices with 0.6-mm collimation. Scan direction was craniocaudal, and the scan volume ranged from the mid pulmonary artery to below the diaphragmatic face of the heart. In all patients, a prospectively electrocardiography (ECG)-triggered axial scan mode was used, triggered at 70% of the R-R interval, with no "padding," which would allow for reconstruction of datasets at other time points within the cardiac cycle.

After placing an 18-gauge intravenous access antecubitally for all patients, contrast agent circulation time (iopromide, 370 mg iodine/ml, Schering, Berlin, Germany) was assessed by application of a test bolus of 10 ml followed by a saline flush of 50 ml at a flow rate of 6 ml/s using a dual-head power injector (CT Stellant, Medrad Inc., Indianola, Pennsylvania). The circulation time was defined by the time between the start of the contrast agent injection and the maximal enhancement in the ascending aorta above the coronary ostia. For angiographic CT data acquisition, a delay that was 2 s longer than the circulation time was used. The

ABBREVIATIONS AND ACRONYMS

CT = computed tomography
DSCT = dual-source computed tomography
ECG = electrocardiography
FBP = filtered back projection
IR = iterative reconstruction
LAD = left anterior descending
LCX = left circumflex
LM = left main
RCA = right coronary artery
ROI = region of interest

From the *Department of Internal Medicine 2 (Cardiology), University of Erlangen, Erlangen, Germany; †Department of Internal Medicine 1 (Cardiology), University of Giessen, Giessen, Germany; ‡Siemens Healthcare, Forchheim, Germany; and the §Department of Radiology, University of Erlangen, Erlangen, Germany. This study was supported by the German government, Bundesministerium für Bildung und Forschung (01EX1012B, Spitzencluster Medical Valley). Dr. Achenbach has received research grants from Siemens Healthcare and Bayer Schering Pharma. Dr. Lell has received research grants from Bayer Healthcare and Siemens Healthcare. Dr. Ropers has received speakers' honoraria and grants from Siemens Healthcare. Dr. Pflederer has received speakers' honoraria from Siemens Healthcare. All other authors have reported that they have no relationships relevant to the contents of this paper to disclose. Pim J. DeFeyter, MD, PhD, served as guest editor.

Manuscript received May 17, 2012; revised manuscript received September 14, 2012, accepted October 1, 2012.

volume of contrast agent injected for the scan was 60 ml using a flow rate of 6 ml/s followed by a 50-ml saline chaser bolus that contained 20% of contrast agent (6 ml/s flow rate).

Image reconstruction. Image reconstruction was performed using both standard filtered back projection (FBP) and IR techniques. For IR, a sinogram-affirmed IR approach (SAFIRE, Siemens Healthcare) was used that applies a noise-modeling technique based on the original raw data. For both FBP and IR, a sharp reconstruction kernel (B46f and I46f), a slice thickness of 0.6 mm, and an increment of 0.4 mm were used. Subsequently, the reconstructed image datasets were transferred to an image-processing workstation (Leonardo, Siemens Healthcare) for further evaluation.

Assessment of image quality. To assess the image quality after FBP and IR, both subjective and objective parameters were evaluated by 2 independent observers who were not made aware of whether the dataset was reconstructed by IR or FBP. First, subjective image quality was assessed after FBP and IR using a 4-point rating score (3 = excellent image quality without any artifacts; 2 = acceptable image quality, not compromising diagnostic vessel assessment; 1 = nondiagnostic image quality for single segments within 1 coronary artery; 0 = nondiagnostic image quality for multiple segments within 1 coronary artery). This rating score was first applied on each coronary artery and subsequently referred to as a mean value of all 4 major coronary arteries (left main artery [LM], left anterior descending artery [LAD], left circumflex artery [LCX], and right coronary artery [RCA]). To obtain objective parameters of image quality of the proximal coronary arteries, image noise and contrast of the proximal coronary arteries as well as contrast-to-noise ratios were determined for both reconstruction methods (FBP and IR) according to previously described methods (17,18). Image noise was defined as the SD of CT density in a region of interest (ROI) placed in the aortic root. To account for anatomic differences between patients, the ROI was chosen as large as possible, while carefully avoiding inclusion of the aortic wall to prevent partial volume effects. In a standardized fashion, the ROI was placed immediately cranial to the left coronary ostium. Attenuation (signal) within the lumen of the proximal coronary arteries was measured by placing ROIs centrally in the LM, LAD, LCX, and RCA. The size of the ROIs in the proximal coronaries were chosen again as large as possible without including parts of the coronary vessel wall. To determine proximal vessel contrast, the CT attenuation in the connective tissue was measured by placing ROIs immediately next to the vessel contour and subsequently determining the difference in CT attenuation between the vessel lumen and surrounding tissue. Individual contrast values for each patient were determined by calculating the mean contrast values of all 4 coronary arteries ([LM + LAD + LCX + RCA]/4). The contrast-to-noise ratio was determined by dividing the mean contrast value by image noise.

Assessment of diagnostic accuracy. One independent experienced observer unaware of the DSCT results analyzed the patients' invasive coronary angiograms. Any luminal narrowing of ≥50% diameter stenosis within a stent as well as in native coronary segments was defined as a significant stenosis. Two standardized projections of the RCA were acquired as well as 4 views of the left coronary artery. If necessary, additional projections were acquired to achieve at least 2 orthogonal projections of each coronary segment. Two independent observers unaware of the results of the invasive angiography evaluated the DSCT datasets after both FBP and IR in random order with respect to the presence of a significant stenosis in native coronary segments as well as in coronary stents by visual assessment (Figs. 1 and 2). If coronary segments or vessels were rated unassessable (image quality score, 0 to 1), they were considered positive (i.e., showing a significant coronary stenosis). Subsequently, results of coronary DSCT angiography were compared with those of the invasive angiography.

Estimation of radiation dose. The estimation of the effective radiation dose associated with the CT examination was based on the dose-length product and calculated with the following formula using a chest-specific conversion coefficient: dose-length product (mGy × cm) × 0.014 (mSv × mGy^{-1} × cm^{-1}) (19).

Statistical analysis. Statistical analyses were performed using SPSS software version 19.02 (SPSS, Inc., Chicago, Illinois). All continuous variables (patient characteristics, radiation dose, image quality parameters) are expressed as mean ± SD or median (25th to 75th percentiles) and compared using an independent Student *t* test for normally distributed data or a Mann-Whitney *U*/Wilcoxon test for non-normally distributed data. Values of $p < 0.05$ were considered statistically significant for all data analyses.

Sensitivity, specificity, positive predictive value, and negative predictive value for the detection of

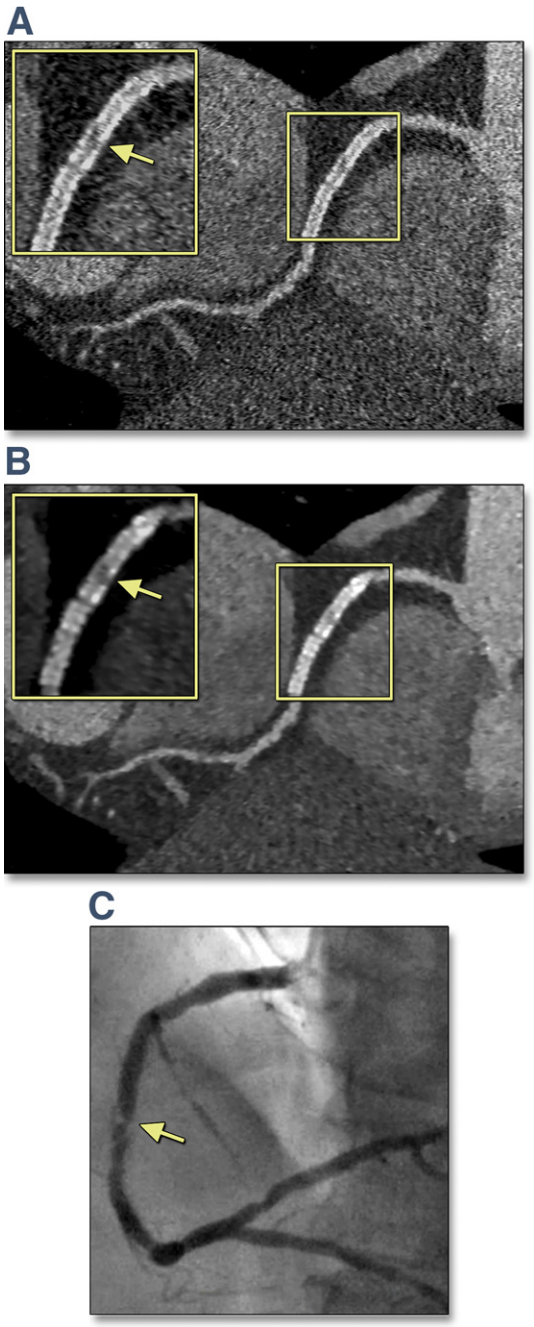

Figure 1. Example of the Presence of In-Stent Restenosis (3.0-mm Diameter Bare-Metal Stent [Coroflex Blue, Braun Vascular Systems, Berlin, Germany])

(A) Filtered back projection dataset with curved multiplanar reconstruction of the right coronary artery (RCA). Diagnosis: the presence of significant in-stent restenosis. **(B)** Iterative reconstruction dataset with curved multiplanar reconstruction of the RCA. Diagnosis: the presence of significant in-stent restenosis. **Boxed areas** clarify the stented segments, **arrows** indicate the in-stent restenosis. **(C)** Corresponding invasive angiogram showing significant luminal narrowing (>50%, **arrow**) within the stent in the mid part of the RCA.

significant in-stent restenosis (≥50% lumen narrowing) were calculated for both the FBP and IR techniques. In addition, a per-patient–based analysis was performed (all unassessable stents were regarded as having in-stent restenosis by DSCT). Sensitivity, specificity, and positive and negative predictive values were also calculated separately for each coronary artery: LM stem, LAD, LCX, and RCA. The diagnostic accuracy of each reconstruction algorithm (FBP and IR) was calculated using the invasive catheterization as the reference method. The diagnostic accuracy of FBP and IR was compared with the use of chi-square statistics.

RESULTS

All 50 coronary DSCT angiography examinations in 9 female and 41 male patients were successfully completed. Patient and scan characteristics are shown in Table 1. The use of prospectively ECG-triggered axial acquisition with a low tube voltage (80 kV) and low tube current (165 mA) resulted in a median dose-length product of 23.0 mGy · cm (22.0; 23.0 mGy · cm), which corresponds to a median estimated effective radiation dose of 0.32 mSv (0.31; 0.32 mSv) only. Forty-one of 50 patients (82%) received beta-blockers, and the heart rate during CT acquisition in the entire cohort was 60 ± 6 beats/min. The stent diameter of all 87 evaluated stents was 3.0 ± 0.4 mm (range 2.5 to 4.0 mm). Thirty-seven of 87 stents were bare-metal stents (Coroflex Blue, Braun AG, Melsungen, Germany), and 50 of 87 stents were drug-eluting stents (Endeavor, Medtronic, Minneapolis, Minnesota) (for further stent characteristics, see Tables 1 and 2).

The application of IR resulted in both a significant improvement of subjective and objective image quality parameters compared with traditional FBPs (Table 3). After use of IR, the subjective image quality score increased from 1.5 ± 0.5 points to 1.8 ± 0.6 points ($p < 0.05$). Although the contrast was not significantly different between FBP and IR, there was a significant difference of the contrast-to-noise ratios (Table 3). This improvement was due to a substantial reduction in image noise by IR compared with FBP (median values, 70 [62; 80] HU for IR vs. 96 [82; 113] HU for FBP; $p < 0.001$).

Objective parameters of image quality showed significantly better values after IR. However, the overall diagnostic accuracy to detect in-stent restenosis was only slightly and not significantly higher after IR (Table 2). Altogether, 26 stents (30%) after FBP and

JACC: CARDIOVASCULAR IMAGING, VOL. 6, NO. 4, 2013
APRIL 2013:458–65

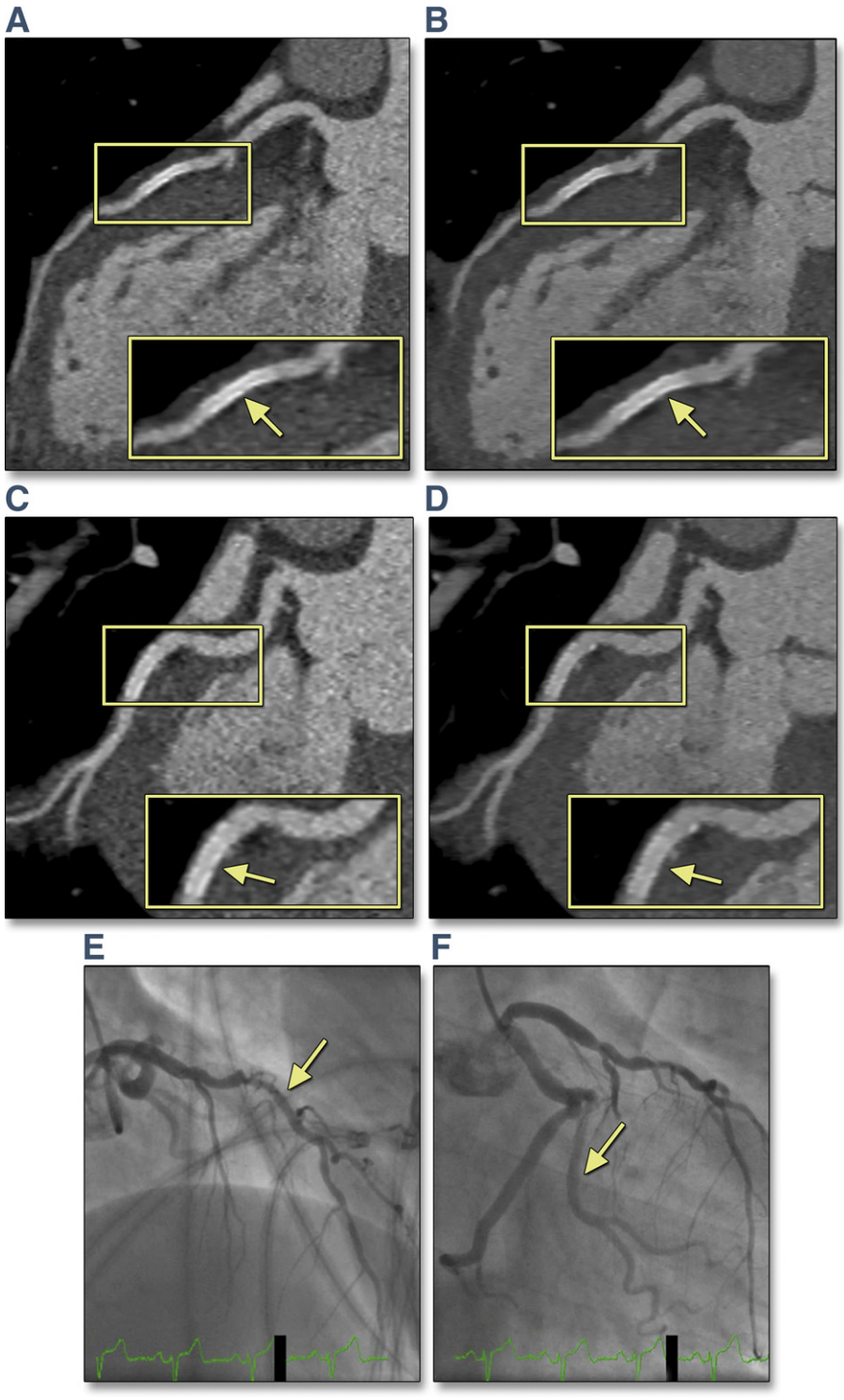

Figure 2. Example of the Absence of In-Stent Restenosis (2 3.0-mm Diameter Bare-Metal Stents [Coroflex Blue, Braun Vascular Systems, Berlin, Germany])

(A, C) Filtered back projection dataset with curved multiplanar reconstruction of the left anterior descending artery (LAD) and left circumflex artery (LCX). Diagnosis: no significant in-stent restenosis. **(B, D)** Iterative reconstruction dataset with curved multiplanar reconstruction of the LAD and LCX. Diagnosis: no significant in-stent restenosis. **Boxed areas** clarify the stented segments, **arrows** indicate the nonobstructive stent lumen. **(E, F)** Corresponding invasive angiogram confirming the absence of significant luminal narrowing within the stents **(arrows)**.

Table 1. Patient, Scan, and Stent Characteristics

Patient and Scan Characteristics	
No. of patients	50
Female patients	9 (18)
Age, yrs	63 ± 10
Mean heart rate, beats/min	60 ± 6
Body mass index, kg/m^2	28.2 ± 3.4
Scan length, mm	137.4 (137.4–137.4)
Dose-length product, mGy · cm	23.0 (22.0–23.00)
Estimated effective dose, mSv	0.32 (0.31–0.32)
Stent Characteristics	
Total no. of stents	87
Mean no. of stents per patient	1.8 ± 0.8
No. of BMSs*	37 (47)
No. of DESs†	50 (63)
Mean diameter of all stents, mm	3.0 ± 0.4

Values are n, n (%), mean ± 1 SD, or median (25th to 75th percentiles). *Coroflex Blue (strut thickness 65 μm), Braun AG, Melsungen, Germany. †Endeavor (strut thickness 91 μm), Medtronic, Minneapolis, Minnesota. BMS = bare-metal stent(s); DES = drug-eluting stent(s).

22 stents (25%) after IR were rated unassessable (no significant difference between FBP and IR) and were therefore classified as having significant in-stent restenosis for further study analysis. Fourteen of 87 stents showed significant in-stent restenosis in invasive coronary angiography. Twelve of all 14 in-stent restenoses could be correctly identified on DSCT after FBP and all 14 in-stent restenoses after IR (Fig. 1), resulting in a sensitivity and specificity of 85% and 69%, respectively, after FBP and 100% and 75%, respectively, after IR for the detection of in-stent stenosis. This trend toward improvement of diagnostic accuracy could also be observed in patient- and vessel-based analyses. Although FBP showed a sensitivity and specificity of 97% and 53%, respectively, for identifying patients with at least 1 significant coronary stenosis (including in-stent restenosis), IR showed corresponding values of 100% and 65%, respectively. On a vessel-based analysis, FBP and IR showed a sensitivity and specificity of 89% and 79% versus 96% and 84%, respectively.

Table 3. Comparison of Image Quality Between Filtered Back Projection and Iterative Reconstruction

Comparison of Image Quality	Filtered Back Projection	Iterative Reconstruction	p Value
4-point rating score	1.5 ± 0.5	1.8 ± 0.6	<0.05
Noise, HU	96 (82–113)	70 (62–80)	<0.001
Contrast, HU	742 (654–877)	783 (707–848)	NS
CNR	8.0 (6.2–9.3)	11.0 (9.6–12.4)	<0.001

Values are mean ± 1 SD or median (25th to 75th percentiles). CNR = contrast-to-noise ratio.

Table 2. Diagnostic Accuracy for the Detection of Significant In-Stent Restenosis After Reconstruction Using Filtered Back Projection and Iterative Reconstruction Compared With Invasive Catheterization

Accuracy	Filtered Back Projection	Iterative Reconstruction
Patient-based analysis		
Sensitivity	97 (32/33) [84–100]	100 (33/33) [89–100]
Specificity	53 (9/17) [28–77]	65 (11/17) [28–86]
PPV	80 (32/40) [64–91]	85 (33/39) [70–94]
NPV	90 (9/10) [56–100]	100 (11/11) [72–100]
Vessel-based analysis		
Sensitivity	89 (43/48) [78–97]	96 (46/48) [86–100]
Specificity	79 (120/152) [72–85]	84 (129/152) [78–90]
PPV	57 (42/74) [45–69]	66 (47/71) [54–78]
NPV	96 (121/126) [91–99]	98 (127/129) [95–100]
Stent-based analysis		
Sensitivity	85 (12/14) [57–98]	100 (14/14) [77–100]
Specificity	69 (51/73) [58–80]	75 (55/73) [64–85]
PPV	32 (11/34) [20–54]	44 (14/32) [26–62]
NPV	96 (51/53) [87–100]	100 (55/55) [94–100]
Unassessable stents	26 (30)	22
Mean diameter of assessable stents, mm	3.2 ± 0.3	3.2 ± 0.3
Mean diameter of unassessable stents, mm	2.7 ± 0.2	2.6 ± 0.2
Unassessable bare-metal stents	8/37 (22)	8/37 (22)
Unassessable drug-eluting stents	18/50 (36)	14/50 (28)

Values are % (n/N) [95% CI], n (%), or mean ± 1 SD. Filtered back projection versus iterative reconstruction: no significant differences according to chi-square test. NPV = negative predictive value; PPV = positive predictive value.

JACC: CARDIOVASCULAR IMAGING, VOL. 6, NO. 4, 2013
APRIL 2013:458–65

DISCUSSION

The present study demonstrates the feasibility of very low-dose CT angiography with use of IR to reliably rule out in-stent restenosis with a high sensitivity and negative predictive value, whereas false-positive diagnoses occur more frequently. As previously shown for the evaluation of coronary artery disease (15,20–22), the use of IR allows a significant reduction of radiation exposure while maintaining diagnostic accuracy. In the present study, the combination of low-dose data acquisition (prospectively ECG-triggered scan, 80 kV, 165 mA) along with IR led to a median estimated effective radiation dose of as little as 0.3 mSv. Compared with images obtained by standard FBP, IR led to a significant improvement of subjective and objective image quality, mainly through the reduction of image noise.

Compared with previous studies that evaluated coronary CT angiography for the detection of in-stent restenosis (1,4,5), IR in the present study shows comparable sensitivity and negative predictive value, but somewhat lower specificity, positive predictive value, and number of assessable stents (26% after IR and 30% after FBP). Obviously, the approach of low-dose data acquisition leads to reduced image quality despite subsequent IR, resulting in more false-positive diagnoses. Furthermore, the inclusion of stents with smaller diameters (<3.0 mm) might have had an additional negative impact on diagnostic accuracy because smaller stent diameters often lead to false-positive diagnoses or result in unassessable datasets (2). Considering the high rate of unassessable stents, even after IR (25%), coronary CT angiography in patients after previous stent implantation remains problematic and should not be recommended on a general basis, especially in stents with smaller diameters. All the same, the ability of coronary CT angiography to reliably rule out in-stent restenosis seems to be maintained. Especially in larger stents, the approach described here may be a clinically feasible one.

The present study was conducted to evaluate IR as a way to lower the radiation dose in CT angiography for the detection of in-stent restenosis. The potential value of IR to enhance diagnostic accuracy in standard acquisitions with higher doses has not been addressed. In this context, other investigators report an improved diagnostic performance of high-resolution coronary CT angiography for the evaluation of coronary stents by the use of IR in ex vivo studies (23). The investigators used IR as a way to decrease noise and partial volume effects in high-resolution images, but not as a way to allow diagnostic image quality in noisy, low-dose datasets. IR as a tool to enhance image resolution also seems to improve diagnostic performance of coronary CT angiography in patients with severely calcified coronary arteries (20).

Study limitations. First, we also included stents with diameters <3.0 mm, which might have affected specificity and positive predictive value. It is not known whether the rate of false-positive diagnoses would have been lower if only larger stents were included for study analysis. Second, we report about a rather small patient population (n = 50) because the study was conducted as a feasibility study of very low-dose coronary CT angiography for the evaluation of coronary stents. In a larger population, the difference between IR and FBP in the accuracy of stenosis detection may have become significant. Third, even though it was not specifically communicated to the observers whether the dataset for analysis was obtained by IR or FBP, the typical appearance of the reconstructed images did not permit true blinding. Therefore, bias, especially concerning subjective rating of image quality, may have been present. Fourth, by using a very low-dose approach leading to significant noise in the datasets, the potential advantages of IR might have been obscured. One might imagine that the use of IR in normal-dose coronary CT angiography might have led to a more significant improvement of stent visualization by reducing blooming artifacts and possibly leading to a lower number of unassessable stents. Future studies will be required to not only compare IR and FBP reconstructions of the same low-dose datasets, but also to elucidate the potential role of IR to enhance diagnostic accuracy to detect in-stent restenosis in normal-dose scans.

CONCLUSIONS

Our study for the first time demonstrates the ability to perform coronary CT angiography for the detection of in-stent stenosis at extremely low radiation exposure. IR leads to a significant improvement of image quality, mainly by reducing image noise. Further studies will be necessary to fully explore the clinical utility of this concept and to clarify the role of IR in datasets acquired at higher doses.

Reprint requests and correspondence: Dr. Tobias Pflederer, Department of Internal Medicine 2 (Cardiology), University of Erlangen, Ulmenweg 18, D-91054 Erlangen, Germany. *E-mail: tobias.pflederer@uk-erlangen.de.*

REFERENCES

1. Kumbhani DJ, Ingelmo CP, Schoenhagen P, Curtin RJ, Flamm SD, Desai MY. Meta-analysis of diagnostic efficacy of 64-slice computed tomography in the evaluation of coronary in-stent restenosis. Am J Cardiol 2009;103:1675–81.
2. Rixe J, Achenbach S, Ropers D, et al. Assessment of coronary artery stent restenosis by 64-slice multi-detector computed tomography. Eur Heart J 2006;27:2567–72.
3. Cademartiri F, Schuijf JD, Pugliese F, et al. Usefulness of 64-slice multislice computed tomography coronary angiography to assess in-stent restenosis. J Am Coll Cardiol 2007;49:2204–10.
4. Pugliese F, Weustink AC, Van Mieghem C, et al. Dual-source coronary computed tomography angiography for detecting in-stent restenosis. Heart 2008;94:848–54.
5. Pflederer T, Marwan M, Renz A, et al. Noninvasive assessment of coronary in-stent restenosis by dual-source computed tomography. Am J Cardiol 2009;103:812–7.
6. Andreini D, Pontone G, Bartorelli AL, et al. Comparison of feasibility and diagnostic accuracy of 64-slice multidetector computed tomographic coronary angiography versus invasive coronary angiography versus intravascular ultrasound for evaluation of in-stent restenosis. Am J Cardiol 2009; 103:1349–58.
7. Hausleiter J, Meyer T, Hermann F, et al. Estimated radiation dose associated with cardiac CT angiography. JAMA 2009;301:500–7.
8. Halliburton SS, Abbara S, Chen MY, et al. SCCT guidelines on radiation dose and dose-optimization strategies in cardiovascular CT. J Cardiovasc Comput Tomogr 2011;5:198–224.
9. Bischoff B, Hein F, Meyer T, et al. Impact of a reduced tube voltage on CT angiography and radiation dose: results of the PROTECTION I study. J Am Coll Cardiol Img 2009;2: 940–6.
10. Earls JP, Berman EL, Urban BA, et al. Prospectively gated transverse coronary CT angiography versus retrospectively gated helical technique: improved image quality and reduced radiation dose. Radiology 2008;246: 742–53.
11. Husmann L, Valenta I, Gaemperli O, et al. Feasibility of low-dose coronary CT angiography: first experience with prospective ECG-gating. Eur Heart J 2008;29:191–7.
12. Achenbach S, Marwan M, Ropers D, et al. Coronary computed tomography angiography with a consistent dose below 1 mSv using prospectively electrocardiogram-triggered high-pitch spiral acquisition. Eur Heart J 2010;31:340–6.
13. Hausleiter J, Meyer T, Hadamitzky M, et al. Radiation dose estimates from cardiac multislice computed tomography in daily practice: impact of different scanning protocols on effective dose estimates. Circulation 2006; 113:1305–10.
14. Leipsic J, Heilbron BG, Hague C. Iterative reconstruction for coronary CT angiography: finding its way. Int J Cardiovasc Imaging 2012;28: 613–20.
15. Moscariello A, Takx RA, Schoepf UJ, et al. Coronary CT angiography: image quality, diagnostic accuracy, and potential for radiation dose reduction using a novel iterative image reconstruction technique-comparison with traditional filtered back projection. Eur Radiol 2011;21:2130–8.
16. Gosling O, Loader R, Venables P, et al. A comparison of radiation doses between state-of-the-art multislice CT coronary angiography with iterative reconstruction, multislice CT coronary angiography with standard filtered back-projection and invasive diagnostic coronary angiography. Heart 2010;96:922–6.
17. Achenbach S, Giesler T, Ropers D, et al. Comparison of image quality in contrast-enhanced coronary-artery visualization by electron beam tomography and retrospectively electrocardiogram-gated multislice spiral computed tomography. Invest Radiol 2003;38:119–28.
18. Ferencik M, Nomura CH, Maurovich-Horvat P, et al. Quantitative parameters of image quality in 64-slice computed tomography angiography of the coronary arteries. Eur J Radiol 2006;57:373–9.
19. Bongartz G, Golding SJ, Jurik AG, et al. European Guidelines for Multislice Computed Tomography. CT quality criteria. Luxembourg: European Commission, Brussels. Available at: http://www.msct.eu/CT_Quality_Criteria.htm. Accessed February 1, 2012.
20. Renker M, Nance JW Jr., Schoepf UJ, et al. Evaluation of heavily calcified vessels with coronary CT angiography: comparison of iterative and filtered back projection image reconstruction. Radiology 2011;260:390–9.
21. Leipsic J, Labounty TM, Heilbron B, et al. Estimated radiation dose reduction using adaptive statistical iterative reconstruction in coronary CT angiography: the ERASIR study. AJR Am J Roentgenol 2010;195:655–60.
22. Leipsic J, Labounty TM, Heilbron B, et al. Adaptive statistical iterative reconstruction: assessment of image noise and image quality in coronary CT angiography. AJR Am J Roentgenol 2010;195:649–54.
23. Min JK, Swaminathan RV, Vass M, Gallagher S, Weinsaft JW. High-definition multidetector computed tomography for evaluation of coronary artery stents: comparison to standard-definition 64-detector row computed tomography. J Cardiovasc Comput Tomogr 2009;3:246–51.

Key Words: coronary CT angiography ■ iterative reconstruction ■ low dose ■ stent.